Supporting Materials

Raman Spectral Dynamics of Single Cells in the Early Stages of Growth Factor Stimulation

Sota Takanezawa, Shin-ichi Morita, Yukihiro Ozaki, and Yasushi Sako

Supplementary Figures

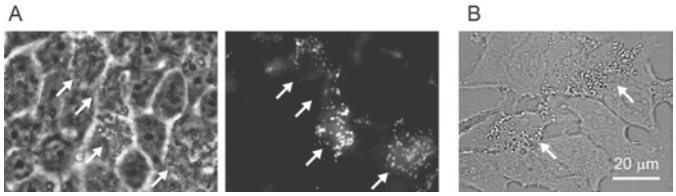

Figure S1. Formation of oil droplets in cells stimulated with HRG for 24 h
(**A**) MCF-7 cells were stained with BODIPY (Invitrogen) using the Adipocyte Fluorescent Staining Kit (Primary Cell. Sapporo, Japan) after HRG stimulation for 24 h. The left picture shows the phase contrast image, and the right picture shows the fluorescence image in the same field of view at wavelengths of 470–490 nm for excitation and 520–550 nm for emission. In the cytoplasm of a small proportion of cells (arrows), bright particles are visible in the phase contrast image. These particles correspond to the oil droplets observed in the fluorescence image. (**B**) Transmission light micrograph of cells after HRG treatment for 24 h. The cells indicated by the arrows contain oil droplets and were classified to the H24c state, which contained large amounts of lipid signals (see text).

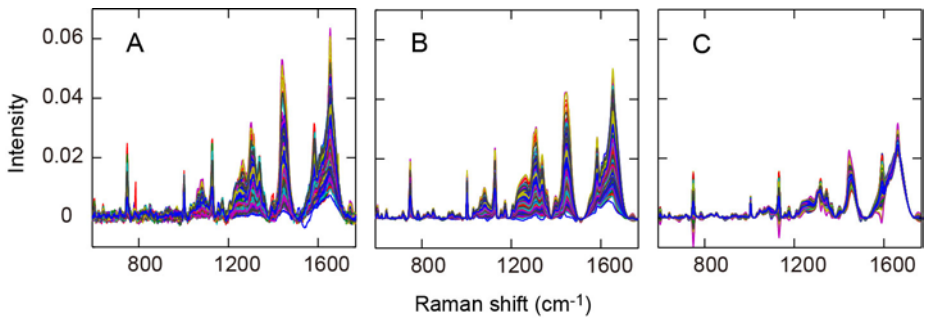

Figure S2. Reconstructed single-cell Raman spectra using PC1 and PC2

The raw spectra after background subtraction (A), and the spectra reconstructed using PC1 and PC2 (B), and PC3 and PC4 (C) are shown. The reconstructed spectra are the sum of the mean of raw spectra and PCs. Variations in the raw spectra that indicate cell-to-cell and time-to-time deviations are largely preserved in the spectra reconstructed using PC1 and PC2, although the sum of the contribution ratios of PC1 and PC2 is only 18.7% (Fig. 2), meaning that the higher-order PCs predominantly contain noise fractions caused by measurement errors and small differences in the specimen, which were eliminated by the reconstruction of the spectra with the major PCs. Spectral variation in PC3 and PC4 is much smaller than those in PC1 and PC2.

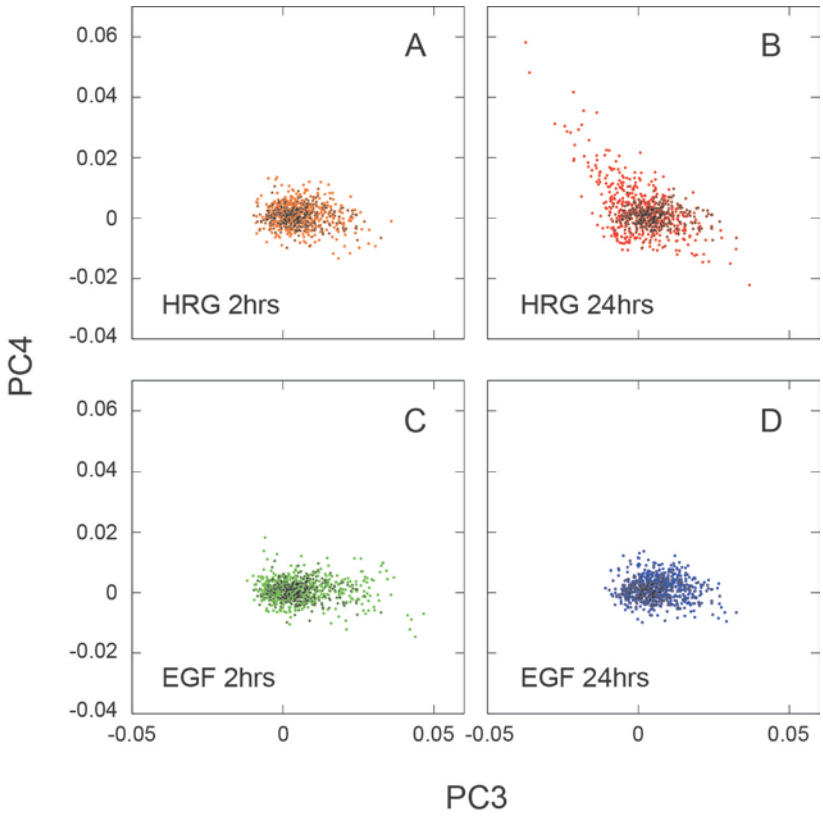

Figure S3. Scores plots in the PC3-PC4 plane

Colored dots indicate the data set of cells under the indicated conditions, and black dots indicate the data set of resting cells for comparison. Most of the spectral distributions are overlapped suggesting the spectral variations derived from random noise. The distribution of spectra after 24h of HRG treatment was enlarged but the center of distribution was not changed significantly from that of the resting cells.

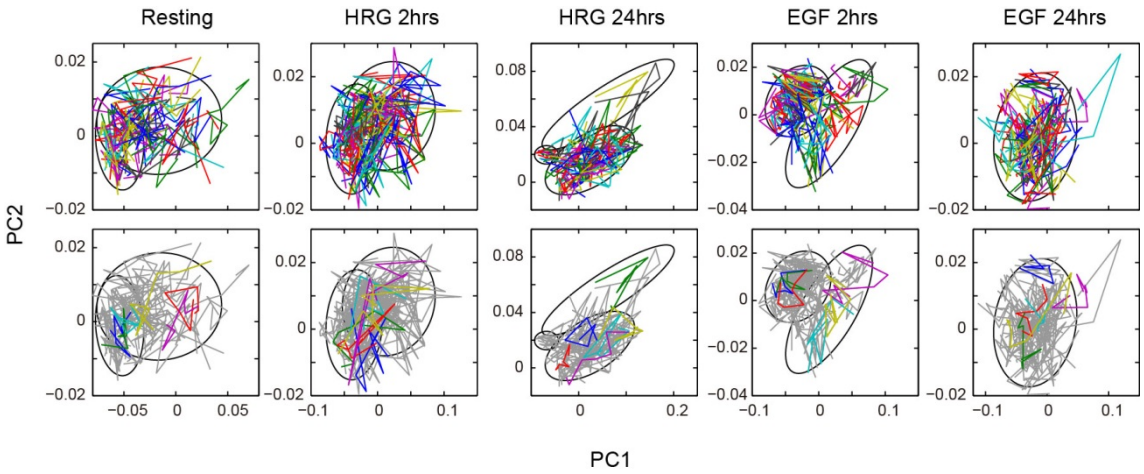

Figure S4. Two-dimensional trajectories of single-cell dynamics

Two-dimensional trajectories of the chemical compositions of single cells are shown in the PC1-PC2 plane. Lines in different colors indicate the trajectories of different single cells. The upper panels show all the trajectories observed, and the lower panels show typical examples. After stimulation of HRG for 2 h, significant numbers of the trajectories moved across the boundaries of the cellular states (ellipses) detected using the Gaussian mixture model (Fig. 4).

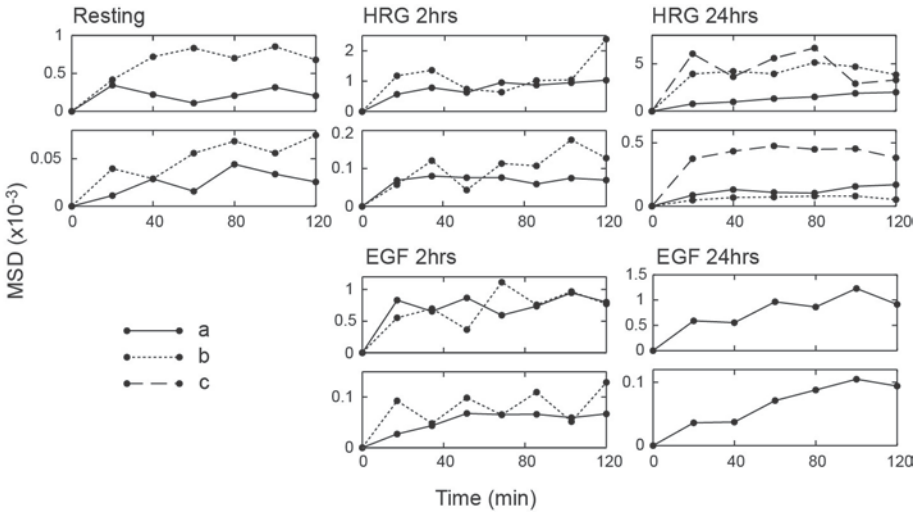

Figure S5. One-dimensional MSD plots of single-cell trajectories in each Gaussian distribution

The upper and lower panels show the time evolution of the MSDs for PC1 and PC2, respectively, for the indicated Gaussian component (Fig. 4). All the plots indicate random diffusion within a restricted area, i.e., the plots do not increase linearly with time but have maximum values to which the plots are asymptotic. This result means that the chemical compositions of single cells fluctuate within a limited region.

Supplementary Tables

Table S1. Raman band assignments of the biomolecules in the cell

Raman Shift (cm^{-1})	DNA/RNA[1]	Proteins[1]	Lipids[1]	Carbohydrates[1]	Cytochrome c[2]
602					resonance Raman
620		C-C twist Phe			
642		C-C twist Tyr			
716			$CN^{+}(CH_3)_3$ str		
748					resonance Raman
782	U, C, T ring br				
810	O-P-O str RNA				
828	O-P-O asym str	ring br Tyr			
852		ring br Tyr			
878			C-C-N+ sym str	C-O-H ring	
936		C-C BK str α-helix	C-O-H glycos		
980		C-C BK str β-sheet	C=H bend		
1002		sym ring br Phe			
1030		C-H in-plane Phe			
1062			skeletal C-C str (All-trans)		
1082	PO_2^{-} str		skeletal C-C str (Gauche)	C-O, C-C str	
1126		C-N str	skeletal C-C str (All-trans)	C-O str	resonance Raman
1156		C-C/C-N str			
1174		C-H bend Tyr			
1208		C-C_6H_5 str Phe, Trp			
1250	T,A	amide III	=CH bend		
1302			CH_2 twist		
1318	G	CH def			
1338	A, G	CH def		CH def	
1448	G, A CH def	CH def	CH def	CH def	
1572	G, A				
1584					resonance Raman
1604		C=C Phe, Tyr			
1616		C=C Tyr, Trp			
1654		amide I	C=C str		
1746			C=O str		

sym, symmetrical; asym, antisymmetrical; BK, backbone; br, breathing; def, deformations; glycos, glycoside bond; in-plane, in-plane deformation; str, stretching

[1] Parker (1983), Takai et al. (1997), Notingher et al. (2004), Huang et al. (2005)

[2]Hu et al. (1993), Ohshima et al (2010)

Table S2. Model selection in Gaussian separation

number of components (k)	1	2	3	4
condition	BIC			
resting	–3784.1	**–3827.3**	–3814.3	–3793.1
HRG 2hrs	–5059.0	**–5081.2**	–5072.8	–5060.7
HRG 24hrs	–3774.8	–3818.5	**–3851.4**	–3841.2
EGF 2hrs	–4998.1	**–5085.6**	–5078.8	–5063.2
EGF 24hrs	**–4460.2**	–4451.5	–4443.3	–4439.3

The minimal numbers are shown in bold font.

References for the Supplement

1. Parker, F. S. 1983. Applications of Infraread, Raman, and Resonance Raman Spectroscopy in Biochemistry. Plenum, New York, NY.

2. Takai, Y., T. Masuko, and H. Takeuchi. 1997. Lipid structure of cytotoxic granules in living human killer T lymphocytes studied by Raman spectroscopy. Biochem. Biophys. Acta. 1335:199–208.

3. Notingher, I., Bisson, I., Bishop, A. E., Randle, W. L., Polak, J. M. P., and Hench, L. L. 2004. In situ spectral monitoring of mRNA translation in embryonic stem cells during differentiation in vitro. Anal. Chem. 76:3185–3193.

4. Huang, Y.-S., T. Karashima, M. Yamamoto, and H. O. Hamaguchi. 2005. Molecular-level investigation of the structure, transformation, and bioactivity of single living fission yeast cells by time- and space-resolved Raman spectroscopy. Biochemistry. 44:10009–10019.

5. Hu, S., I. K. Morris, J. P. Singh, K. M. Smith, and T. G. Spiro. 1993. Complete assignment of cytochrome c resonance Raman spectra via enzymatic reconstitution with isotopically labeled heme. J. Am. Chem. Soc. 115:12446–12458.

6. Ohshima, Y., H. Shinzawa, T. Takenaka, C. Fujita, and H. Sato. 2010. Discrimination analysis of human lung cancer cells associated with histological type and malignancy using Raman spectroscopy. J. Biomed. Opt. 15:017009 (1–8).